Article

Design and Synthesis of Biotinylated Bivalent Carboline Derivatives as Potent Anti-tumor Agents

Xueyuan Chen, Yi Zheng, Songlin Song, Ying Liu, Yi Wang, Yong Huang, Xiaoyi Zhang, Meng Zhang, Ming Zhao, Yuji Wang, and Li Li

J. Org. Chem., **Just Accepted Manuscript** • DOI: 10.1021/acs.joc.0c01067 • Publication Date (Web): 18 Aug 2020

Design and Synthesis of Biotinylated Bivalent Carboline Derivatives as Potent Anti-tumor Agents

Xueyuan Chen, Yi Zheng, Songlin Song, Ying Liu, Yi Wang, Yong Huang, Xiaoyi Zhang, Meng Zhang, Ming Zhao, Yuji Wang,* Li Li*

Beijing Area Major Laboratory of Peptide and Small Molecular Drugs; Engineering Research Center of Ministry of Education of China; Beijing Laboratory of Biomedical Materials; School of Pharmaceutical Sciences, Capital Medical University, Beijing 100069, P.R. China

* E-mail: wangyuji@ccmu.edu.cn (Y. Wang).

* E-mail: renulee@ccmu.edu.cn (L. Li).

Supporting Information

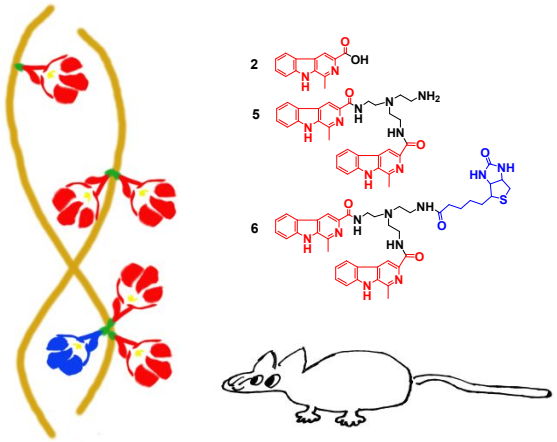

ABSTRACT: Compound **6**, a novel *β*-carboline comprising two 1-methyl-9*H*-*β*-carboline-3-carboxylic acids and a biotin moiety conjugated together using tris(2-aminoethyl)amine, was synthesized and tested for its cytotoxicity towards MCF-7 and HepG2 cell lines, and anti-tumor potency in an S180 tumor bearing mouse model. Compound **6** was delivered via biotin receptor-mediated endocytosis, and exerted its therapeutic effects by intercalation binding with DNA. *In vivo* anti-tumor evaluations of **6** found it to be efficacious, and of low systemic toxicity.

INTRODUCTION

Peganum harmala. L is a perennial, herbaceous plant which has been used in Chinese folk medicines to treat alimentary tract cancers for hundreds of years.[1] β-Carboline alkaloids isolated from *Peganum harmala* can induce apoptosis and inhibit tumor cell proliferation, and have recently attracted attention for their potential anti-tumor activities.[2-4] β-Carboline alkaloids exert their anti-tumor effects via multiple mechanisms, including DNA intercalation and inhibition of topoisomerases I and II; cyclin-dependent kinase (CDK); and IkK kinase complex (IkK).[5] As DNA intercalators, their planar aromatic moieties insert between adjacent base pairs, which decreases the DNA helical twist and length of the DNA strand, and disrupts important processes such as DNA replication, transcription and repair.[6] Recently, many DNA intercalators have been used as potential lead compounds due to their inhibitory effect on the growth of cancer cells.[7,8] Also, bivalent ligands formed by the tethering of two DNA intercalating agents by an appropriately designed spacer have proved more effective inhibitors than their corresponding monomers by increasing the number of binding sites and improving the interactions of ligands with their corresponding receptors.[9-11] We recently reported a bivalent ligand based on isoquinoline-3-carboxylic acid exhibited improved anti-tumor activity, compared to isoquinoline-3-carboxylic acid alone.[12]

β-carboline alkaloid derivatives are interesting synthetic targets due to their medicinal importance. [13] In synthetic organic chemistry we generally seek to develop novel synthetic route that can make new compounds. However, when chemistry addresses disease problems, the chemistry must be considered in the context of biological system, such as cellular system, or even whole animal.[14] There is a great demand for expanding the availability of β-carboline-containing synthetic building blocks to promote medicinal chemistry research.[15] When β-carboline derivatives are used as anti-tumor agents, the lack of tumor specificity leads to relatively high dose administration. Therefore, the synthetic strategies varied accordingly.

One possible solution to this problem is the conjugation of therapeutic agents with targeting ligands whose receptors are over-expressed on the surface of cancer cells. Receptor-mediated internalization would result in their selective delivery at high doses.[16] Biotin has attracted much attention as a potential targeting ligand due to its relatively simple chemical structure and low molecular weight, and the very high demands of cancer cells for biotin compared to normal cells. Receptors for biotin such as avidin and its bacterial counterpart streptavidin are present on the membranes of cancer cells, and biotin can form stable complexes with both. Consequently, biotin or biotin-conjugates should be assimilated by cancer cells through receptor-mediated endocytosis at higher rates than normal cells. [17,18]

We previously reported that the conjugation of 1-methyl-9H-β-carboline-3-carboxylic acid **2** (Scheme 1) with amino acid benzylesters can increase the *in vitro* anti-proliferation and *in vivo* anti-tumor activities of **2**.[19] The conjugation of two of 1-methyl-9H-β-carboline-3-carboxylic acid units with a biotin moiety in the same molecule was suggested as a possible strategy to reduce the *in vivo* treatment dose and improve the therapeutic index of **2**. To test this idea, we constructed a new bivalent ligand **6** bearing a biotin moiety based on 1-methyl-9H-β-carboline-3-carboxylic acid. Compound **6** comprises two 1-methyl-9H-β-carboline-3- carboxylic acid pharmacophores; biotin; and the tris(2-aminoethyl) amine (TREN) linker. This concept was supported by the therapeutic effect of compound **6** *in vitro* and *in vivo* bioactivity evaluations.

RESULTS AND DISCUSSION

Scheme 1 depicts our synthesis of **6**. Compound **1**, obtained by Pictet-Spengler reaction of tryptophan and acetaldehyde, was hydrolyzed in the presence of sodium hydroxide to give compound **2** in 91% yield. Mono-N-Boc-protected TREN **3**,[20] obtained from the reaction of TREN with di-tert-butyldicarbonate in 74% yield, was condensed with compound **2** in 1:2 stoichiometry by DMTMM (4-(4,6-dimethoxy-1,3,5-triazin

-2-yl)-4-methyl morpholinium chloride) to give the compound **4** in 14% yield. Compound **4** was treated with TFA to remove the Boc protecting group, giving compound **5** in 29% yield. The conjugation of compound **5** with biotin-NHS ester afforded the desired compound **6** in 29% yield.

Scheme 1. Synthesis of Compound 6

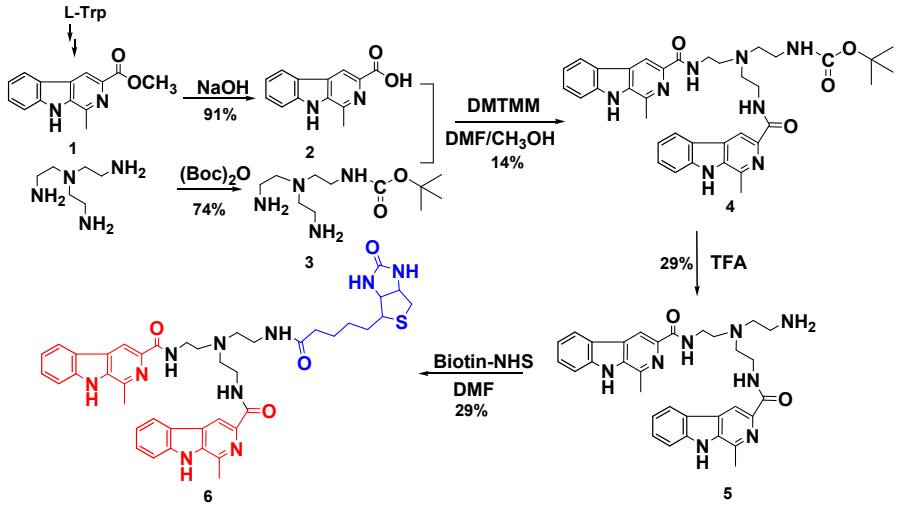

UV-visible absorption titration studies were used to study the binding behavior of compound **6** with DNA, figure S1. Upon the addition of calf thymus DNA (CT-DNA) to a solution of compound **6** in Tris-HCl buffer at pH 7.4, the characteristic absorption peaks corresponding to compound **6** (3.0×10^{-5} mol/L) were seen to gradually decrease in intensity, accompanied by a bathochromic shift of about 19 nm at the absorption maximum (267 nm). This hypochromic effect and bathochromic shift are thought to arise from intercalating binding between compounds **6** and CT-DNA.[8] The binding constant K_b between compound **6** and CT-DNA was estimated to be 9.7×10^4 M^{-1}according to the Scatchard equation.[21] As the CT-DNA and compound **6** have an overlapping UV-vis absorption band, the corresponding CT-DNA was added to the reference cuvette to compensate for the control absorbance.

DNA-antitumor agent intercalation binding plays an important role in cell proliferation,[7] and is able to

induce DNA conformational changes. It is known that the CD (circular dichroism) spectra of the B-form of DNA has a positive band at about 275 nm due to base stacking, and a negative band of similar magnitude at about 245 nm due to base right-hand helixity.[22] In order to verify if compound **6** could induce DNA conformational changes, the CD spectrum of CT-DNA in Tris-HCl buffer was recorded. It was found that the negative band intensities of CT-DNA (100 μM) gradually decreased with increasing concentrations of compound **6** (0, 10, 20 μM) at 245 nm, while only subtle differences were seen to the band at 275 nm (Figure S2). The decrease in band intensity at 245 nm may arise from the insertion of compound **6** into the DNA, resulting in the uncoupling and elongation of DNA double helix, and a decrease in the DNA helicity.[23] Thus, the results of the CD spectrum analysis together with the UV-visible spectra verify the intercalative mode of binding of compound **6** into CT-DNA helix.

The binding specificity of biotinylated **6** to avidin was investigated in an avidin-HABA competitive binding assay.[24] HABA (2-(4'-hydroxyazobenzene) benzoic acid) is an orange dye, capable of binding to avidin in the same pocket used to bind biotin. HABA has a maximum UV absorbance at 350 nm; and the non-covalent complex of avidin/HABA displays a new UV-visible absorbance band at 500 nm. The intensity of this characteristic absorbance reduces upon addition of biotin, since biotin has much a stronger affinity for avidin compared with HABA, and thus easily displaces the HABA from the avidin/HABA complex. This displacement can be quantitatively monitored by the absorbance decrease at 500 nm. The avidin/HABA complex was titrated with biotinylated **6**, and the data are shown in the overlaid UV-vis spectra (Figure 1). Upon addition of biotinylated **6**, the absorbance at 500 nm decreased and the shade of orange color of complex faded with an increase in the molar ratio of biotinylated compound **6** to avidin, suggesting the avidin/HABA complex is displaced by biotinylated **6.** There was no further absorbance decrease until the molar ratio of biotinylated **6** to avidin reached four, where upon the color of the complex remained constant

(Figure S3). Thus, the binding stoichiometry of biotinylated **6** to avidin is four, which is the same stoichiometry as unmodified biotin (biotin: avidin = 4:1) and consistent with literature reports.[25] These results constitute evidence that **6** can form stable complex with avidin, and therefore **6** is able to selectively target the biotin receptors over-expressed on the cancer cells membrane surface.

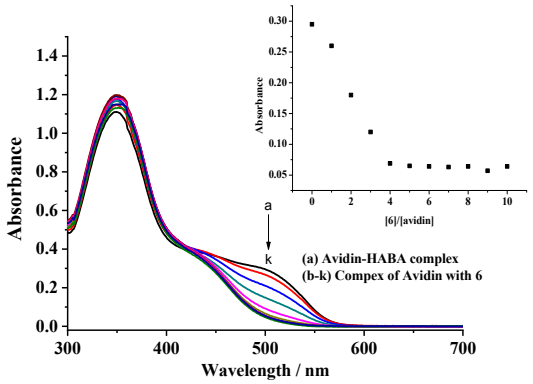

Figure 1. UV/vis spectra of the avidin-HABA complex upon additions of biotinylated **6**([**6**]/[avidin] = 0 ~ 10) in buffer solution (pH = 7.4). Inserted: Absorption changes of avidin-HABA complex at 500 nm upon the addition of **6**.

To evaluate the anti-tumor potency of compound **6**, its *in vitro* cytotoxic activity against a selection of different cancer cell lines was ascertained using the MTT assay.[26] The biotin receptor-expressing cell lines MCF-7 and HepG2 were treated with varying concentrations of compound **6** for 72 h. Doxorubicin (DOX) was used as positive control (IC_{50} = 0.16 ± 0.02 μM for MCF-7 and 0.58 ± 0.06 μM for HepG2 at 48 h), compounds **2** and **5** were used as references. Due to the low aqueous solubility of **2**, it was found to be inactive above 100 μM. Cell viability graphs (Figure 2A) show that the tested compounds reduced MCF-7 and HepG2 viability at 72 h after seeding, in a concentration-dependent manner ($P < 0.05$). For instance, the cell viability of compound **6** at 155 μM was ca. 45% in HepG2 cells over 72 h, while the cell viability of compound **5** was ca 62% at the same concentration. It is evident that the compound **6** displays higher cytotoxicity compared with the compound **5** against the biotin receptor-positive cancer cell lines tested

(MCF-7 and HepG2 cells), within a concentration range of 40 to 225 μM, as shown in Figure 2A. The MCF-7 cell line was more sensitive to compound **6** than the HepG2 cell line, showing that compound **6** was a more potent inhibitor of the growth of this cell line. However, biotin free compound **5** and biotinylated compound **6** separately exhibited no significantly different cytotoxicity against the biotin receptor-negative cancer line HCT-116 ($P > 0.05$) within all tested concentration ranges. These results demonstrate that biotinylated compound **6** accomplished the selective delivery of 1-methyl-9H-β-carboline-3-carboxylic acid pharmacophores into biotin receptor-positive cancer cells over biotin receptor-negative cells.

To further verify the role of biotin in receptor-mediated endocytosis, the biotin competitive MTT assay was performed. When HepG2 cells were pre-incubated with an excess of biotin (100 μM) for 24 h, the biotin receptors of HepG2 cells became occupied. The reduced *in vitro* cytotoxic activity of compound **6** against biotin-treated HepG2 cells compared to the biotin-untreated HepG2 cells at all tested concentrations indicated the competitive binding of biotinylated **6** with the biotin receptors of HepG2 cells was prevented or reduced. Moreover, the difference in cytotoxic activity of compound **5** against biotin-treated and biotin-untreated HepG2 cells was not significantly ($P > 0.05$), as shown in Figure 2B. The results of the competitive MTT assay [27] constitute evidence that the biotinylated compound **6** could be targeted to the surface of cancer cells via biotin receptor-mediated endocytosis, accumulate with a higher dose, and exhibit more potent activity, compared to compound **5**.

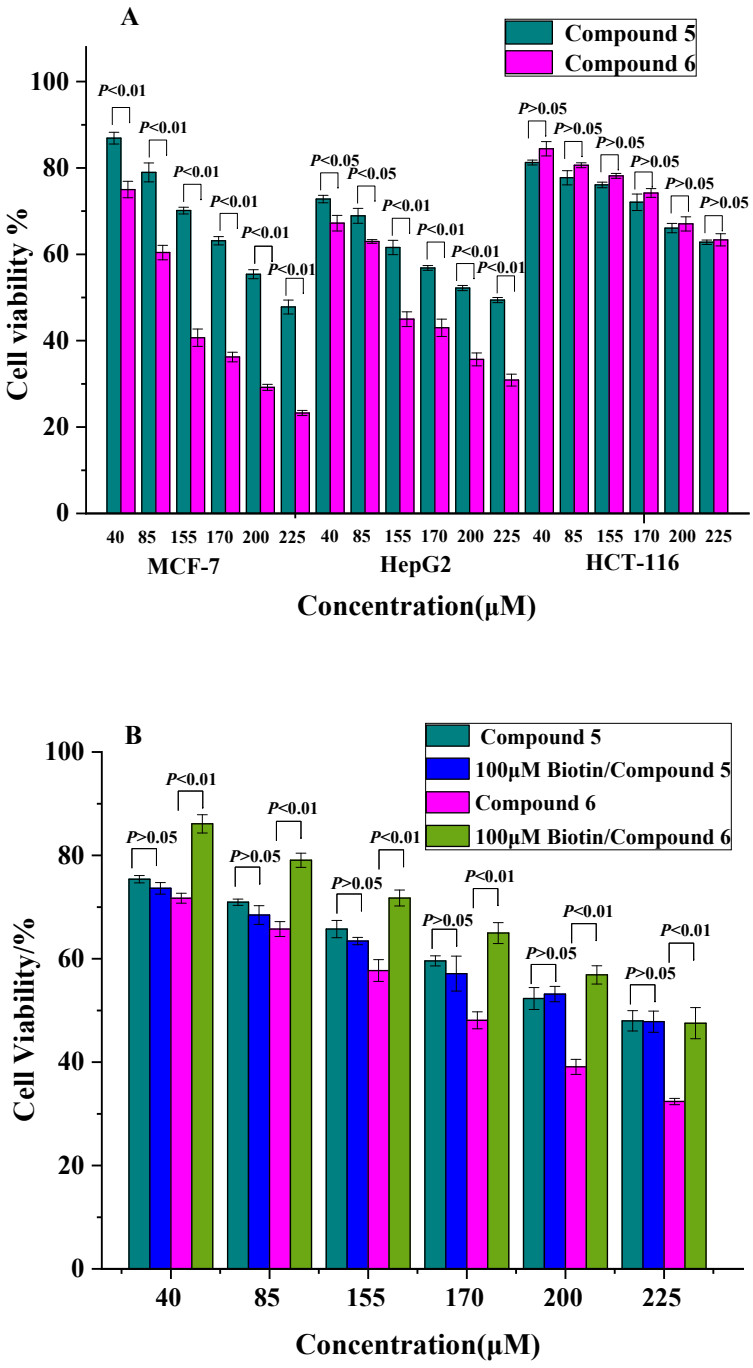

Figure 2. (A) Cell viability for biotin receptor-positive MCF-7, HepG2 cell lines, and biotin receptor-positive cancer line HCT-116. (B) Cell viability of HepG2 cell without and with pretreatment with excess of biotin (100 μM).

Apoptosis-induced cell death can alter cell nuclear morphology, which can be visualized by confocal laser scanning microscopy.[28] To examine the morphology of the HepG2 cells, they were stained blue with

4'-6-diamidino-2-phenylindole (DAPI). It was observed that the morphology of the nuclei of the cells treated with compound **6** became abnormal, containing condensed and irregular patterns of chromatin distribution, after 24 h of exposure (Figure 3). With a further increase in the concentration of compound **6** to 225 μM, the number of apoptotic cells with condensed nuclei increases. The similar phenomenon was observed for positive control DOX, which also reported the nuclear accumulation of cancer cell following exposure to DOX.[29] On the other hand, cells treated with negative control NS (normal saline) and biotin free **5** showed no or fewer nuclear morphological changes.

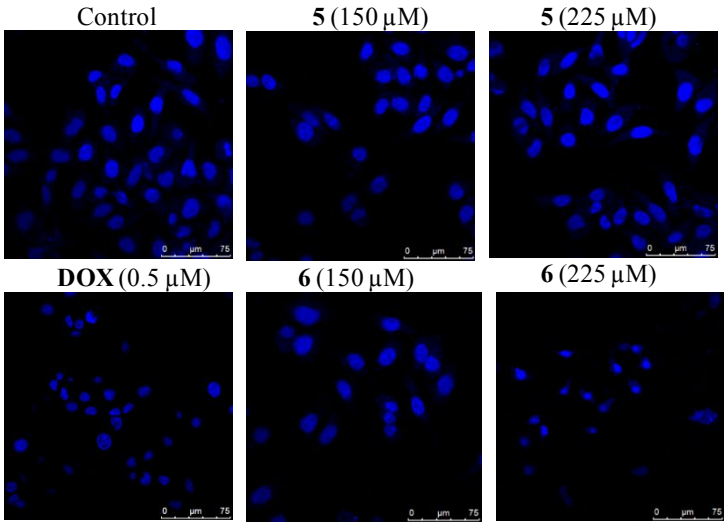

Figure 3. Confocal microscopy of HepG2 cells treated with indicated concentration of **5**, **6** and DOX. The non-treated and treated cells were stained with DAPI and observed by confocal microscopy. Scale bar = 75 μm.

The percentage of apoptotic HepG2 cells was determined by monitoring the translocation of phosphatidylserine from the inner face of the plasma membrane to the cell surface using the Annexin V-FITC apoptosis detection kit. HepG2 cells treated with **6** (0, 150 μM and 225 μM, respectively) were evaluated for apoptosis by Annexin-V FITC/PI double staining followed by flow cytometry, doxorubicin (DOX, 0.5 μM) was used as positive control. HepG2 cells, which were harvested in the absence of compound **6**, were ~100% viable (negatively stained, lower left quadrant of the cytogram). When HepG2

cells were treated with 150 μM compound **6**, the percentage of early apoptotic cells (annexin-V positive and propidium iodide negative, lower right quadrant) and cells in the late stages of apoptosis (annexin-V and propidium iodide positive, upper right quadrants) increased to 12.6% in Figure 4. Upon increasing concentration of **6** to 225 μM, the percentage of apoptotic cells further increased to 17.1%. However, the percentage of necrotic cells (upper left) did not increase with the increasing concentration of **6**. These results indicate that HepG2 cells underwent the early and late stages of apoptosis after treatment with **6**. The increased percentage of apoptotic cells of **6** is consistent with the increased anti-proliferative activity of **6** compare to **5**.

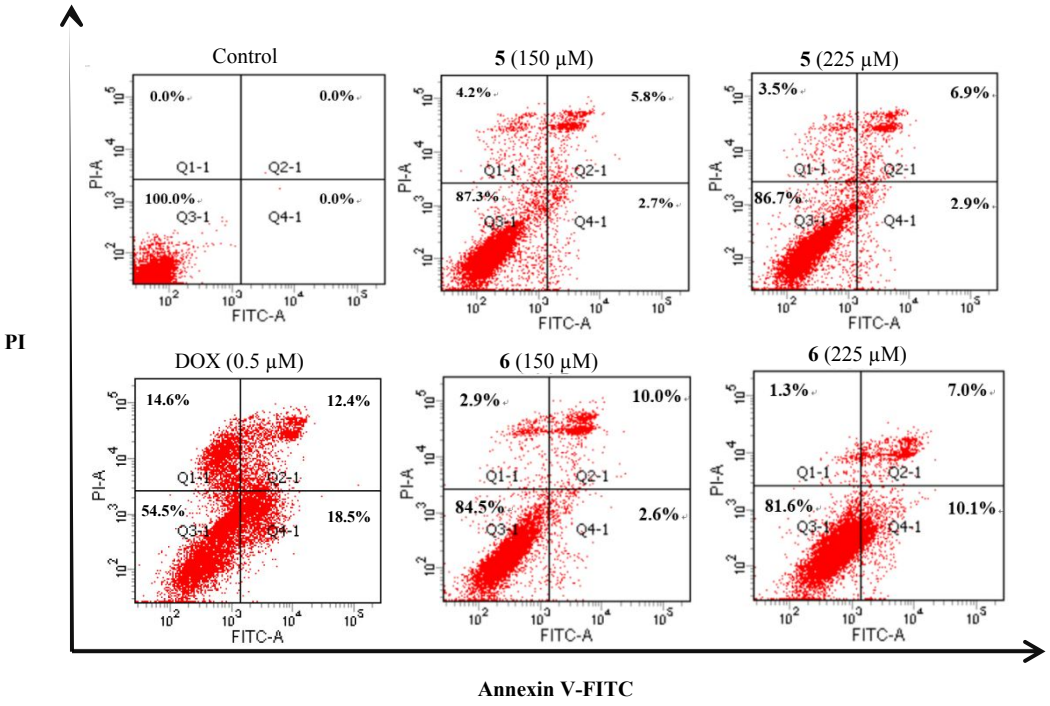

Figure 4. HepG2 cells were treated with the indicated concentration of **5, 6** and DOX for 24 h, and stained with FITC-Annexin V and PI, followed by flow cytometry analysis.

The therapeutic potential of **6** *in vivo* was evaluated using the S180 tumor bearing mouse model.[12] Twenty-four hours after implantation, the mice were randomized into groups of 5 with 10 in each group. Normal saline (NS, 10 mL/kg) and doxorubicin (DOX, 2 μmol/kg) were used as a negative and positive

control, respectively. Test agents were administered every day at the indicated doses for 10 days. All animals were sacrificed on the twelfth day. The activity was represented by tumor weight. The tumor weights of the mice receiving DOX at dose of 2 μmol/kg (0.62 ± 0.17 g); compound **2** at dose of 8 μmol/kg (1.31 ± 0.26 g); compound **5** at dose of 2 μmol/kg (1.09 ± 0.32 g); and compound **6** at dose of 0.2 μmol/kg (0.93 ± 0.20 g), were significantly lower than those of the mice receiving NS (2.09 ± 0.47 g), table S1. This shows that DOX and the test agents all display anti-tumor activity at the treatment doses. As shown in Figure 5, the *in vivo* anti-tumor activity of compound **5** at dose of 2 μmol/kg was comparable to that compound **2** at dose of 8 μmol/kg. This implies that *in vivo* the effective dose of compound **5** was four times lower than that of compound **2**. The improved anti-tumor potency of **5** compared to **2** could be due to an increased local concentration of pharmacophore associated with **5**, due to the bivalent approach. To examine the role of biotin in the enhancement of drug uptake at the tumor, the pharmacokinetics of compounds **5** and **6** were evaluated in S180 tumor bearing mice.[30] Test compounds were introduced by a single tail vein injection. Dose ratio of compound **5** to **6** in pharmacokinetic study was the same to the dose ratio in *vivo* evaluation. Plasma levels of tested compounds were monitored over time using an LC-MS/MS system. As shown in Figure S4, compound **6** displayed a similar pharmacokinetic profile to that of biotin free compound **5**. These results indicated that the therapeutic effectiveness of the mice administered compound **6** at lower dose compared with those administered compound **5** was caused by biotin mediated uptake. The biotin receptor-mediated **6** maintained the higher pharmacophore accumulation to reach the tumor site. Thus, **6** exerted an equivalent therapeutic effect at a dose ten times lower than that of biotin free bivalent ligand **5**. It is noteworthy that **6** exhibited better anti-tumor activity than **2** at 1/40 of the dose of compound **2** ($P < 0.01$).

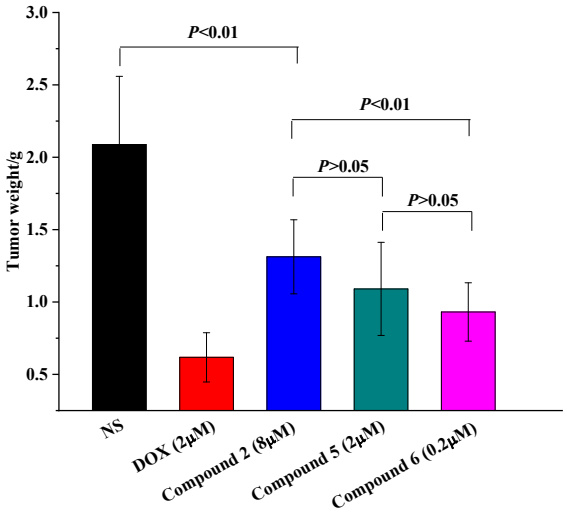

Figure 5. Tumor weights of S180 mice treated with the indicated doses of test agents, n =10.

The body weights of mice receiving test agents were monitored for 10 consecutive days. In Figure S4, the body weight gain of the mice receiving DOX was suppressed throughout the 10 days. Conversely, mice treated with compounds **2**, **5** and **6** achieved similar levels of weight gain as compared with the NS treatment group (body weights consistently increased from ~ 22 g to ~ 32 g). The organ to body weight ratio of liver and spleen were significantly decreased in the DOX group in Figure S5. In contrast, the organ to body weight ratios of treatment with compound **6** were not significantly different with that of NS. These results suggest that compound **6** did not affect body weights, organ to body weight ratio to mice at the treatment dose, which suggests it was not toxic at that dose.[31]

CONCLUSION

In summary, compound **6**, a novel anti-tumor agent comprising two 1-methyl-9*H*-*β*-carboline-3-carboxylic acids as double pharmacophores, biotin as a targeting ligand, and TREN as the bridging moiety, has been designed, synthesized, and tested *in vitro* against biotin receptor-positive MCF-7 and HepG2 cell lines, and *in vivo* in an S180 tumor bearing mouse model. *In vivo* evaluations of **6** found it to be efficacious at 1/40 of the dose of compound **2**, and of low systemic toxicity. Its superior performance compared with

reference compound **2** is thought to arise from the preferential delivery of **6** to cancer cells due to the over-expression of biotin receptors on the cancer cell surface, with which the biotin moiety of **6** can interact. After endocytosis, compound **6** exerts its therapeutic effects by intercalation binding with the DNA. Accordingly, compound **6** is proposed as a new anti-tumor lead compound.

EXPERIMENTAL SECTION

General Information. All coupling and deprotection reactions were carried out under anhydrous conditions and under a positive pressure of nitrogen, unless otherwise stated. 1-Methyl-9H-*β*-carboline-3-carboxylate (**1**),[19] 1-methyl-9H-*β*-carboline-3-carboxylic acid (**2**),[19] mono-N-Boc-protected TREN (**3**),[20] and biotin NHS ester were synthesized as previously described. [32] Avidin from egg white (avidin), and HABA (2-(4'-hydroxyazobenzene) benzoic acid) were purchased from Sigma (Shanghai,China). All pH values were obtained using pH paper, unless otherwise stated. ESI-MS experiments were performed on a Quattro micro API™ and Bruker micrOTOF-Q ™, and Fourier transform ion cyclotron resonance (FT-ICR, 9.4T solariX, Bruker, US) with dual ion source of ESI/matrix-assisted laser desorption ionization ESI-MS, respectively. ^{1}H NMR spectra were recorded on a Bruker Avance-500 MHz. ^{13}C NMR spectra were recorded on a Bruker Avance-125 MHz and 75 MHz. HPLC was performed on a Shimadzu LC30AD equipped with UV and fluorescence detectors. Phenomenex Luna Omega C18 100A 1.6 µm × 50 × 2.1 mm, Cloumn Number: 144, eluting with 80% water containing 0.1% FA (formic acid) + 20% acetonitrile containing 0.1% FA. Statistical analyses of all the biological data were carried out using use of analysis of variance (ANOVA). *P*-values < 0.01 were considered statistically significant, *P*-values > 0.05 were considered not differ significantly.

Tert-butyl 2-(bis(2-(1-methyl-9H-pyrido[3,4-b]indole-3-carboxamido)ethyl)amino)ethyl)carbamate(4). DMTMM (4-(4,6-dimethoxy-1,3,5-triazin-2-yl)-4-methylmorpholinium chloride) (0.80 g, 2.92 mmol) and

NMM (N-methylmorpholine) (2 mL) were added dropwise to a solution of **2** (0.66 g, 2.92 mmol) and mono-N-Boc-protected TREN (**3**) **(**0.30 g, 1.22 mmol**)** in DMF (30 mL) at room temperature, with stirring, until the pH of the resulting mixture was about 9, the pH value was checked by pH paper. Then solution was diluted with methanol (2 mL) and allowed to stir at room temperature. After 18h, the solvent was removed *in vacuo* and the residue was dissolved in ethyl acetate. After removal of solvent the crude product was purified by column chromatography using silica gel (EtOAc:MeOH = 8:2). The product **4** (0.11 g， 14%) was obtained as a white solid. TLC (EtOAc:*i*-Pro:NH_3 = 15:1:0.1), R_f = 0.3. Mp: 252-254°C. ^{1}H NMR (300 MHz, DMSO-d_6): δ/ppm = 12.11 (s, 2H), 8.66-8.62 (m, 4H), 8.29 (d, J = 7.5 Hz, 2H), 7.61-7.51 (m, 4H), 7.25 (t, J = 7.5 Hz, 2H), 6.67 (s, 1H), 3.48-3.46 (m, 4H), 3.10-3.08 (m, 2H), 2.72-2.76 (m, 10H), 2.64-2.66 (m, 2H), 1.31-1.23 (m, 9H). ^{13}C{^{1}H} NMR (75MHz, DMSO-d_6) δ/ppm = 165.3, 141.3, 139.5, 136.3, 128.5, 127.8, 122.4, 121.8, 120.2, 112.7, 112.2, 63.5, 54.1, 37.7, 28.6, 20.8. ESI-TOF (m/z): Calc for $C_{37}H_{41}N_8O_4^-$, ([M-H]$^{-1}$): 661.3251, found: 661.3358.

N,N'-(((2-Aminoethyl)azanediyl)bis(ethane-2,1-diyl))bis(1-methyl-9H-pyrido[3,4-b]indole-3-carboxamide) (5).

Compound **4** (0.33 g, 0.50 mmol) was dissolved in TFA (4 mL). The solution was agitated for 6 h. The TFA was evaporated off under reduced pressure at room temperature. The residue was dissolved in $NH_3{\cdot}H_2O$ (0.3-0.4 mL) to get a pH of about 7. After removal of the solvent, the crude product was purified by column chromatography using silica gel and CH_2Cl_2: MeOH: NH_3 (10: 1: 0.2). The product **5** (0.08 g, 29%) was obtained as a pale yellow solid. TLC (CH_2Cl_2: MeOH: NH_3 =10: 1: 0.2), R_f = 0.29. Mp: 242-243°C. ^{1}H NMR (500 MHz, DMSO-d_6): δ/ppm =11.73 (s, 2H), 8.64 (t, J = 5.0 Hz, 2H), 8.63 (s, 2H), 8.26 (d, J = 10.0 Hz, 2H), 7.54-7.50 (m, 4H), 7.23-7.25 (m, 2H), 3.49 (d, J = 5.0 Hz, 4H), 2.73 - 2.76 (m, 4H), 2.66-2.70 (m, 8H), 2.61-2.62 (m, 2H). ^{13}C{^{1}H} NMR (125 MHz, DMSO-d_6) δ/ppm = 165.1, 141.1, 139.5, 136.1, 128.6,

127.7, 122.4, 121.8, 120.2, 112.5, 112.1, 58.2, 53.9, 37.6, 20.7. HR-MS (FT-MS) (m/z): Calc for $C_{32}H_{33}N_8O_2^-$, ($[M-H]^{-1}$): 561.2726, found: 561.2756.

N,N'-(((2-(5-(2-oxohexahydro-1H-thieno[3,4-d]imidazol-4-yl)pentanamido)ethyl)azanediyl)bis(ethane-2,1-diyl))bis(1-methyl-9H-pyrido[3,4-b]indole-3-carboxamide) (6).

Compound **5** (0.16 g, 0.29 mmol) was added to a solution of biotin-NHS ester (0.12 g, 0.35 mmol) in dry DMF (4 mL). The reaction mixture was stirred at room temperature for 17 h. The solvent was then removed in vacuo, and the crude product was purified by column chromatography using silica gel (CH_2Cl_2: MeOH: NH_3=10: 1: 0.1). Product **6** (0.06g, 29%**)** was obtained as a white solid. TLC (CH_2Cl_2: MeOH: NH_3 =10: 1: 0.1), R_f = 0.29. Mp: 204-205°C. ^{1}H NMR (500 MHz, DMSO-d_6): δ/ppm = 11.76 (s, 2H), 8.59-8.62 (m, 4H), 8.26-8.25 (m, 2H), 7.63 (t, J = 5.0 Hz, 1H), 7.51-7.56 (m, 4H), 7.22-7.26 (m, 2H), 6.36 (s, 1H), 6.30 (s, 1H), 4.21 (t, J = 5.0 Hz, 1H), 3.99 (t, J = 5.0 Hz, 1H), 3.46-3.48 (m, 4H), 3.22-3.23 (m, 2H), 3.18 (d, J = 5.0 Hz, 1H), 2.87-2.91 (m, 1H), 2.76 (t, J = 5.0 Hz, 4H), 2.70-2.73 (m, 6H), 2.64-2.67 (m, 2H), 2.54 (s, 1H), 2.03 (t, J = 7.5 Hz, 2H), 1.33-1.53 (m, 4H), 1.04-1.22 (m, 2H). ^{13}C{^{1}H} NMR (125 MHz, DMSO-d_6) δ/ppm = 172.4, 165.4, 163.2, 141.2, 141.2, 139.6, 136.2, 128.6, 127.8, 122.4, 121.9, 120.3, 112.6, 112.2, 61.5, 59.7, 55.8, 54.2, 53.9, 49.1, 37.8, 37.7, 35.7, 28.7, 28.5, 25.7, 20.7. HR-MS (FT-MS) (m/z): Calc for $C_{42}H_{49}N_{10}O_4S^+$, ($[M+H]^{+1}$): 789.3659, found: 789.3631.

UV-visible absorption titrations.

UV-visible absorption titrations were performed using a UV–Vis spectrophotometer (UV-2550, Shimadzu) at 25 °C using 1 cm path length quartz cuvette. The CT-DNA stock solution was prepared by dissolving CT-DNA in Tris buffer (pH = 7.40, C = 0.1 mol/L). If the ratio of absorbance at 260 and 280 nm, A260/A280, was greater than 1.8, the CD-DNA solution was considered to be sufficiently free from protein. The concentration of CT-DNA stock solution was determined by Lambert-Beer law using the absorption

coefficient at 260 nm (6600 M^{-1}•cm^{-1}). The stock solution was stored at 4 ºC and used within 4 days.

The binding constant K_b between compound **6** and CT-DNA was estimated as 5.0×10^4 M^{-1} according to the Scatchard equation.[21]

$$[DNA]/(\varepsilon_a - \varepsilon_f) = [DNA]/(\varepsilon_b - \varepsilon_f) + 1/K(\varepsilon_b - \varepsilon_f)$$

Where [DNA] is the concentration of CT-DNA in base pairs; and ε_a , ε_f and ε_b correspond to the apparent extinction coefficient for A_{obsd}/[**6**], the extinction coefficient for the free compound, and the extinction coefficient for the compound in the fully bound form, respectively. The binding constant K_b was obtained from the slope and intercept of the plot of $[DNA]/(\varepsilon_a - \varepsilon_f)$ versus [DNA].

Circular dichroism (CD) studies.

Circular dichroism (CD) spectra were recorded with Jasco J-810 spectrometer at 25 °C using a 1 mm quartz sample cell. Wavelength scans were acquired from 200 nm to 400 nm at 1 nm bandwidth, with a scanning speed of 100 nm/min. All CD experiments were carried out in Tris-HCl buffer (pH = 7.40, C = 0.1 mol/L) upon addition of 0, 10, 20 μmol/L of compound **6** onto 100 μmol/L of CT-DNA, respectively.

Biotin binding: HABA assay. [24]

The binding specificity of **6** towards avidin was investigated by HABA (2-(4'-hydroxyazobenzene) benzoic acid) assay in Tris-HCl buffer solution (pH = 7.40, C = 0.1 mol/L, 1% DMSO).The HABA assay was used to determine the extent of biotinylation. Avidin solution (3.7×10^{-6} mol/L, 9.0 mL), and HABA solution (2.0×10^{-3} mol/L, 0.5 mL) were combined to afford a stock solution (C_{avidin}= 3.5×10^{-6} mol/L, C_{HABA} = 1.0×10^{-4} mol/L). Different concentrations of compound **6** of ($0 \sim 3.5 \times 10^{-5}$ mol/L) were added into the stock solution. The final value was 1.0 mL. HABA dye is bound to avidin and displays a new UV-visible absorbance at 500 nm. This characteristic absorbance was reduced upon addition of **6**. The corresponding **6** was added to the reference cuvette to compensate for the control absorbance.

***In vitro* antiproliferation assay.**

The cytotoxicities of compounds **5** and **6** against biotin receptor-positive cancer cell lines MCF-7 (human breast adenocarcinoma), HepG2 (human hepatocellular liver carcinoma), and biotin receptor-negative cancer cell lines HCT-116 (human colorectal cancer) were separately studied using the MTT assay.[26] A suspension of cells (100 μL of 5×10^5 cells/mL) was seeded in 96-well plates and incubated at 37ºC in a humidified atmosphere of 5% CO_2 for 4 h. The medium was replaced by medium containing different concentrations of test samples in PBS containing 5‰ DMSO and tests were in triplicates. Incubation was carried out at 37 ºC in an incubator supplied with 5% CO_2 for 72 h. Following incubation, 25 μL of 5 mg/mL of MTT were added to each well and the plate was put back in the incubator for another 4 h at 37 ºC. Then culture medium was removed. The resulting MTT-formazan product was dissolved in 100 μL DMSO. The amount of formazan was determined by measuring the optical density at 570 nm. The cytotoxic activities were observed to occur in a dose-dependent manner in the cells. The activity was expressed as cell viability, which is the percentage of living cells in the total cells.

Biotin competitive MTT assay [27]

A suspension of HepG2 cells (100 μL of 2×10^3 cells/mL) was seeded in 96-well plates and incubated at 37ºC for 4 h in a humidified atmosphere of 5% CO_2, until the cells were fully attached. 100 μM Biotin were pre-incubated into HepG2 cells for 24 h. After the medium was removed, and washed three times with PBS, the different concentrations of compounds were added to the medium and incubated for another 72 h. The cytotoxicities were determinted according to MTT assays.

Confocal microscopy imaging: Identification of apoptotic cells by DAPI Staining.

HepG2 cells (2×10^5 cells/mL) were seeded in confocal dish with pore size of 20 mm and were cultured in an incubator at 37 °C under an atmosphere of 5% CO_2 for 4 h. The cells were then washed with

PBS, fixed with 4% paraformaldehyde and permeabilized with 0.1 % Triton X-100. The cells were incubated for 10 min in the dark with DAPI (10 μg/mL). Cells were washed again with PBS and finally sealed with 50% glycerin. The stained cells were viewed by laser scanning confocal microscope (Leica TCS SP8, Germany).

Apoptosis assay.

Apoptosis of HepG2 cells was detected using the Annexin V-FITC Apoptosis Detection Kit. HepG2 cells, in log phase of growth, were seeded at a density of 2×10^5 cells/mL in a 6-well cell culture plate. The cells were cultured in an incubator at 37 °C under an atmosphere of 5% CO_2. After the cells were attached, the original medium in the cell plate was discarded, and different concentrations of the compound in medium were added. The cells were collected by adding EDTA-free trypsin after 24 hours culture, and the cells were washed three times with PBS (centrifuge at 2000 rpm for 5 min) to collect 5×10^5 cells. The cells were resuspended in 500 μL of 1X Binding Buffer. After addition 5 μL of annexin V-FITC and 5 μL of propidium iodide (PI, optional), the cells were incubated at room temperature for 5 min in the dark. The assay was performed using a flow cytometer (LSR Fortessa). Fluorescence was measured with an excitation wavelength of 488 nm through FL-1 (525 nm) and FL-3 filters (620 nm).

***In vivo* anti-tumor study.**

All studies described herein were performed under a review protocol approved by the ethics committee of Capital Medical University. The committee was assured that the welfare of the animals was maintained in accordance to the requirements of the animal welfare act and according to the guide for care and use of laboratory animals. The *in vivo* antitumor potency was determined using ICR mice (Swiss, 6-8 weeks old, 20.00 ± 2.00 g weight) inoculated with S_{180} sarcoma. S_{180} ascites tumor cells were used to form solid tumors after subcutaneous injection. For initiation of subcutaneous tumors, the cells were obtained in their anascitic

form from the tumor-bearing mice, which were serially transplanted once per week. Subcutaneous tumors were implanted by injecting 0.2 mL of 0.9% saline containing 1.2×10^7 viable tumor cells under the skin on the right armpit. 24 hours after implantation, the mice were randomly divided into five experimental groups with 10 in each group, and treated with normal saline (NS, 10 mL/kg), DOX (2 μmol/kg), compound **2** (8 μmol/kg), compound **5** (2 μmol/kg) and compound **6** (0.2 μmol/kg) for 10 consecutive days. The weights of the mice were recorded every day. Twenty-four hours after the last administration, all mice were weighed, sacrificed (diethyl ether anesthesia), and immediately dissected. The tumor, heart, liver, spleen, kidney, and brain of each mouse were weighed.

Pharmacokinetics

For plasma: 10 μL standard samples in duplicate, samples in triplicate, and mouse plasma samples were mixed with 60 μL acetonitrile containing IS (200 ng/mL of tolbutamide, 50 ng/mL of propranolol and 500 ng/mL of Dic) in EP tubes. After the mixture was vortexed for 1 min, then centrifuged for 10 min (13000 rpm, 4℃), transfer 50 μL supernatant to a 96-well plate with 150 μL pure water, shake for 10 min and finally inject 10 μL into LC-MS/MS system.

ASSOCIATED CONTENT

Supporting Information

The Supporting Information is available free of charge on the ACS Publications website.

NMR, MS, UV and CD spectra; the effect of compound **6** on the body weight and organ-to-body weight ratio of S180 mice (file type, i.e., PDF).

AUTHOR INFORMATION

Corresponding Authors

* E-mail: wangyuji@ccmu.edu.cn (Y. Wang).

* E-mail: renulee@ccmu.edu.cn (L. Li).

ORCID

Y. Wang: 0000-0003-3842-7627
L. Li: 0000-0002-2244-3967

ACKNOWLEDGMENT

This work was supported by Beijing Natural Science Foundation (2172018), Great Wall Scholar Project of Beijing Municipal Education Commission (CIT&TCD20180332), and 863 Programme 2015AA020902.

REFERENCES

(1) Cao, R.; Peng, W.; Wang, Z.; Xu, A. *β*-Carboline Alkaloids: Biochemical and Pharmacological Functions. *Curr. Med. Chem*. **2007**, 14, 479−500.

(2) Spindler, A.; Stefan, K.; Wiese, M. Synthesis and Investigation of Tetrahydro-*β*-carboline Derivatives as Inhibitors of the Breast Cancer Resistance Protein (ABCG2). *J. Med. Chem*. **2016**, 59, 6121−6135.

(3) Li, S. G.; Wang, K. B.; Gong, C.; Bao, Y.; Qin, N. B.; Li, D. H.; Li, Z. L.; Bai, J.; Hua, H. M. Cytotoxic Quinazoline Alkaloids from the Seeds of Peganum Harmala. *Bioorg. Med. Chem. Lett*. **2018**, 28, 103–106.

(4) (a) Karan, D.; Dubey, S.; Pirisi, L.; Nagel, A.; Pina, I.; Choo, Y. M.; T Hamann, M. The Marine Natural Product Manzamine A Inhibits Cervical Cancer by Targeting the SIX1 Protein. *J. Nat. Prod*. **2020**, 83, 286–295. (b) He, L.; Liao, S.Y.; Tan, C. P.; Lu, Y. Y.; Xu, C. X.; Ji, L. N.; Mao, Z W. Cyclometalated Iridium (III)-*β*-Carboline Complexes as Potent Autophagy-Inducing Agents. *Chem. Commun*. **2014**, 50, 5611–5614.

(5) Wang, K. B.; Li, D. H.; Hu, P.; Wang, W. J.; Lin, C.; Wang, J.; Lin, B.; Bai, J.; Pei, Y. H.; Jing, Y.-K.; Li, Z. L.; Yang, D. Hua. H. M. A Series of *β*-Carboline Alkaloids from the Seeds of Peganum Harmala show G-Quadruplex Interactions. *Org. Lett*. **2016**, 18, 14, 3398–3401.

(6) Hurley, L.H. DNA and Its Associated Processes as Targets for Cancer Therapy. *Nat. Rev*. **2002**, 2, 188–200.

(7) (a) Brana, M.F.; Cacho, M.; Garcia, M.A.; de Pascual-Teresa, B.; Ramos, A.; Dominguez, M.T.; Pozuelo, J.M.; Abradelo, C.; Rey-Stolle, M. F.; Yuste, M.; Banez-Coronel, M.; Lacal, J. C. New Analogues of Amonafide and Elinafide, Containing Aromatic Heterocycles: Synthesis, Antitumor Activity, Molecular Modeling, and DNA Binding Properties. *J. Med. Chem.* **2004**, 47, 1391–1399. (b) Zhang, H.; Li, R.; Ba, S.; Lu, Z.; Pitsinos, E. N.; Li, T.; Nicolaou, K. C. DNA Binding and Cleavage Modes of Shishijimicin A. *J. Am. Chem. Soc*. **2019**, 141, 7842–7852.

(8) Sun, Y. G.; Sun, D.; Yu, W.; Zhu, M. C.; Ding, F.; Liu, Y. N.; Gao, E. J.; Wang, S. J.; Xiong, G.; Dragutan, I.; Dragutan. V. Synthesis, Characterization, Interaction with DNA and Cytotoxicity of Pd(II) and Pt(II) Complexes Containing Pyridine Carboxylic Acid Ligands. *Dalton Trans*. **2013**, 42, 3957–3967.

(9) Sheng, R.; Sun, H.; Liu, L.; Lu, J.; McEachern, D.; Wang, G.; Wen, J.; Min, P.; Du, Z.; Lu, H.; Kang, S.; Guo, M.; Yang, D.; Wang, S. A Potent Bivalent Smac Mimetic (SM-1200) Achieving Rapid, Complete, and Durable Tumor Regression in Mice. *J. Med. Chem*. **2013**, 56, 3969–3979.

(10) (a) Rice, D. R.; Clear, K. J.; Smith, B. D. Imaging and Therapeutic Applications of Zinc(II)-Dipicolylamine Molecular Probes for Anionic Biomembranes. *Chem. Commun*. **2016**, 52, 8787–8801. (b) Dai, J.; Dan, W.; Schneider, U.; Wang, J. *β*-Carboline Alkaloid Monomers and Dimers: Occurrence, Structural Diversity, and Biological Activities. *Eur. J. Med. Chem*. **2018**, 157, 622–656.

(11) Qian, M.; Wouters, E.; Dalton, J. A. R.; Risseeuw, M. D. P.; Crans, R. A. J.; Stove, C.; Giraldo, J.; Craenenbroeck, K. V.; Calenbergh. S. V. Synthesis Toward Bivalent Ligands for the Dopamine D_2 and Metabotropic Glutamate 5 Receptors. *J. Med. Chem*. **2018**, 61, 8212–8225.

(12) Gao, F.; Liu, H.; Li, L.; Guo, J.; Wang, Y.; Zhao, M.; Peng, S. Design, Synthesis, and Testing of an Isoquinoline-3-Carboxylic-Based Novel Anti-Tumor Lead. *Bioorg. Med. Chem. Lett.* **2015**, 25, 4434–4436.

(13) Karan,D.; Dubey,S.; Pirisi, L.; Nagel,A.; Pina,I.; Choo,Y.-M.; Hamann,M. T. The Marine Natural Product Manzamine A Inhibits Cervical Cancer by Targeting the SIX1 Protein. *J. Nat. Prod*. **2020**, 83, 2, 286–295.

(14) (a) Hruby, V. J. Organic Chemistry and Biology: Chemical Biology Through the Eyes of Collaboration. *J. Org. Chem*. **2009**, 74, 9245–9264. (b) Ojima, I. Exploration of Fluorine Chemistry at the Multidisciplinary Interface of Chemistry and Biology. *J. Org. Chem*. **2013**, 78, 6358−6383.

(15) (a) Wang, Z.-X.;Xiang,J.-C.; Cheng,Y.; Ma,J.-T.; Wu,Y.-D.; Wu,A.-X. Direct Biomimetic Synthesis of *β*-Carboline Alkaloids from Two Amino Acids. *J. Org. Chem*. **2018**, 83, 19, 12247–12254. (b) Kumar, K.; Wang, P.; Wilson, J.; Zlatanic, V.; Berrouet, C.; Khamrui, S.; Secor, C.; Swartz, E. A.; Lazarus, M.; Sanchez, R.; Stewart, A. F.; Garcia-Ocana, A.; DeVita, R. J. Synthesis and Biological Validation of a Harmine-Based, Central Nervous System (CNS)-Avoidant, Selective, Human *β*-Cell Regenerative Dual-Specificity Tyrosine Phosphorylation-Regulated Kinase A (DYRK1A) Inhibitor. *J. Med. Chem.* **2020**, 63, 6, 2986–3003.

(16) (a) Mathew, G.; Hannan, A.; Hertzler-Schaefer, K.; Wang, F.; Feng, G. S.; Zhong, J.; Zhao, J. J.; Downward, J.; Zhang, X. Targeting of Ras-mediated FGF Signaling Suppresses Pten-Deficient Skin Tumor. *Proc. Natl. Acad. Sci. U.S.A.* **2016**, 113, 13156–13161. (b) Srinivasarao, M.; Galliford, C. V.; Low.P. S. Principles in the Design of Ligand-Targeted Cancer Therapeutics and Imaging Agents. *Nat. Rev. Drug. Discov*. **2015**, 14, 203–219. (c) Jiang, X.; Bugno, J.; Hu, C.; Yang, Y.; Herold, T.; Qi, J.; Chen, P.; Gurbuxani, S.; Arnovitz, S.; Strong, J.; Ferchen, K.; Ulrich, B.; Weng, H.; Wang, Y.; Huang, H.; Li, S.; Neilly, M. B.; Larson, R. A.; Le Beau M. M.; Bohlander, S. K.; Jin, J.; Li, Z.; Bradner, J. E.; Hong, S.; Chen, J. Eradication of Acute Myeloid Leukemia with FLT3 Ligand-Targeted miR-150 Nanoparticles. *Cancer Res*. **2016**, 76, 4470–4480.

(17) (a) Ren, W. X.; Han, J.; Uhm, S.; Jang, Y.; Kang, C.; Kim, J. H.; Kim, J. S. Recent Development of Biotin Conjugation in Biological Imaging, Sensing, and Target Delivery. *Chem. Commun*. **2015**, 51, 10403–10418. (b) Plażuk, D.; Zakrzewski, J.; Salmain, M.; Błauż, A.; Rychlik, B.; Strzelczyk, P.; Bujacz, A.; Bujacz, G. Ferrocene-Biotin Conjugates Targeting Cancer Cells: Synthesis, Interaction with Avidin, Cytotoxic Properties and the Crystal Structure of the Complex of Avidin with a Biotin-Linker-Ferrocene Conjugate. *Organometallics* **2013**, 32, 5774–5783.

(18) (a) Deshpande, N. U.; Jayakannan, M. Biotin-Tagged Polysaccharide Vesicular Nanocarriers for Receptor-Mediated Anticancer Drug Delivery in Cancer Cells. *Biomacromolecules* **2018**, 19, 3572−3585. (b) Wang, J. T.; Wang, L.; Ji, X.; Liu, L.; Zhao, H. Synthesis of Zwitterionic Diblock Copolymers with Clevable Biotin Groups at the Junction Points and Fabrication of Bioconjugtes by Biotin-Streptavidin Coupling. *Macromolecules* **2017**, 50, 2284−2295.

(19) Wu, J.; Zhao, M.; Qian, K.; Lee, K. H.; Morris-Natschke, S. L.; Peng, S. Novel N-(3-Carboxyl-9-benzyl-*β*-Carboline-1-yl)ethylamino Acids: Synthesis, Anti-tumor Evaluation, Intercalating Determination, 3D QSAR Analysis and Docking Investigation. *Eur. J. Med. Chem*. **2009**, 44, 4153–4161.

(20) DiVittorio, K. M.; Hofmann, F. T.; Johnson, J. R.; Abu-Esba, L.; Smith, B. D. Facilitated Phospholipid Translocation in Vesicles and Nucleated Cells Using Synthetic Small Molecule Scramblases. *Bioorg. Med. Chem.* **2009**, 17, 141–148.

(21) Kim, Y. R.; Gong, L.; Park, J.; Jang, Y. J.; Kim, J.; Kim, S. K. Systematic Investigation on the Central Metal Ion Dependent Binding Geometry of M-meso-Tetrakis(N-methylpyridinium-4-yl)porphyrin to DNA and Their Efficiency as an Acceptor in DNA-Mediated Energy Transfer. *J. Phys. Chem. B*. **2012**, 116, 2330–2337.

(22) Balaz, M.; Steinkruger, J. D.; Ellestad, G.A.; Berova, N. 5'-Porphyrin-Oligonucleotide Conjugates: Neutral Porphyrin-DNA Interactions. *Org. Lett*. **2005**, 7, 5613–5616.

(23) Li, X.; Lin, Y.; Wang, Q.; Yuan, Y.; Zhang, H.; Qian, X. The Novel Anti-Tumor Agents of 4-Triazol-1,8-Naphthalimides: Synthesis, Cytotoxicity, DNA Intercalation and Photocleavage. *Eur. J. Med. Chem*. **2011**, 46, 1274–1279.

(24) Qi, K.; Ma, Q.; Remsen, E. E.; Clark, C. C., Jr.; Wooley, K. L. Determination of the Bioavalability of Biotin Conjugated onto Shell Cross-Linked (SCK) Nanoparticles. *J. Am. Chem. Soc.* **2004**, 126, 6599−6607.

(25) (a) Kuan, S. L.; Bergamini, F. R. G.; Weil, T. Functional Protein Nanostructures: a Chemical Toolbox. *Chem*. *Soc*. *Rev*. **2018**, 47, 9069-9105. (b) Liu, W.; Samanta, S. K.; Smith, B. D.; Isaacs, L. Synthetic Mimics of Biotin/(Strept)avidin. *Chem Soc. Rev.* **2017**, 46, 2391–2403.

(26) Al-Allaf, T. A. K.; Rashan, L. J. Synthesis and Cytotoxic Evaluation of the First Trans-Palladium(II) Complex with Naturally Occurring Alkaloid Harmine. *Eur. J. Med. Chem*. **1998**, 33, 817–820.

(27) Yu, G.; Cook, T. R.; Li, Y.; Yan, X.; Wu, D.; Shao, L.; Shen, J.; Tang, G.; Huang, F.; Chen, X.; Stang, P. J. Tetraphenylethene-Based Highly Emissive Metallacage as a Component of Theranostic Supramolecular Nanoparticles. *Proc. Natl. Acad. Sci. U.S.A.* **2016**, 113, 13720–13725.

(28) Yadav, K.; Rao Meka, P. N.; Sadhu, S.; Guggilapu, S. D.; Kovvuri, J.; Kamal, A.; Srinivas, R.; Devayani, P.; Babu, B. N.; Nagesh, N. Telomerase Inhibition and Human Telomeric G-Quadruplex DNA Stabilization by a *β*-Carboline-Benzimidazole Derivative at Low Concentrations. *Biochemistry* **2017**, 56, 4392–4404.

(29) Xi, J.; Li, M.; Jing, B.; An, M.; Yu, C.; Pinnock, C. B.; Zhu, Y.; Lam, M. T.; Liu. H. Long-Circulating Amphiphilic Doxorubicin for Tumor Mitochondria-Specific Targeting. *ACS Appl. Mater. Interfaces* **2018**, 10, 43482−43492.

(30) McRae Page, S.; Henchey, E.; Chen, X.; Schneider, S.; Emrick, T. Efficacy of PolyMPC-DOX Prodrugs in 4T1 Tumor-Bearing Mice. *Mol. Pharmaceutics* **2014**, 11, 1715−1720.

(31) Liu, J.; Mengel, K.; Friedberg, K. D. *In vivo* Effects of Fluconazole on Lymphocyte Subpopulations of the Thymus and Spleen in Mice: Flow Cytometry Analysis. *Int. J. Immunopharmacol*. **1996**, 18, 449–457.

(32) Li, K.; Chen, Y.; Li, S.; Nguyen, H. G.; Niu, Z.; You, S.; Mello, C. M.; Lu, X.; Wang, Q. Chemical Modification of M13 Bacteriophage and Its Application in Cancer Cell Imaging. *Bioconjugate Chem.* **2010**, 21, 1369–1377.